*Work supported in part by the U. S. Atomic Energy Commission under Contract No. AT(11-1)-3505.

†N. S. F. Senior Post Doctoral Fellow. Permanent address: Stevens Institute of Technology, Hoboken, N. J.

‡Permanent address: New York University, New York, N. Y.

[1]See, e.g., J. Freeman *et al.*, in *Proceedings of the International Conference on Weak Interactions, Argonne, 1965* (Argonne Natl. Lab., Argonne, Ill., 1966).

[2]M. A. B. Bég, J. Bernstein, and A. Sirlin, Phys. Rev. Letters 23, 270 (1969). See also D. Dicus and R. Norton, Phys. Rev. D 1, 1360 (1970).

[3]See, e.g., E. Abers, D. Dicus, R. Norton, and H. Quinn, Phys. Rev. 167, 1461 (1968).

[4]K. Wilson, Phys. Rev. 179, 1499 (1969).

[5]K. Johnson and F. E. Low, Progr. Theoret. Physics (Kyoto) Suppl. 37–38, 74 (1966); J. D. Bjorken, Phys. Rev. 148, 1467 (1966).

[6]See, e.g., S. L. Adler and W. K. Tung, Phys. Rev. D 1, 2846 (1970).

[7]Dicus and Norton, Ref. 2.

[8]Cf. L. Durand *et al.*, Phys. Rev. 130, 1188 (1963).

[9]See also M. A. B. Bég, in *Brookhaven National Laboratory Lectures in Science* (Gordon and Breach, New York, 1970), Vol. 5; A. Sirlin, Ann. Phys. (N.Y.) 61, 294 (1970).

[10]A. Sirlin (unpublished). The exact result of one of the two integrals of Eq. (A2), namely,

$$J_1 \equiv \frac{8i}{(2\pi)^2}\int \frac{d^4k}{k^2-\lambda_{\min}^2+i\epsilon} \times \frac{1}{k^2+2l\cdot k+i\epsilon}\,\frac{1}{k^2+2p\cdot k+i\epsilon},$$

was given in R. E. Behrends, R. J. Finkelstein, and A. Sirlin, Phys. Rev. 101, 866 (1956) [see Eq. (7a) *et seq.*].

[11]More precisely, the error is $O(Z\alpha(l/M)\ln(l/M))$ or $O(Z\alpha(l/M))$, where l in these expressions stands for the positron energy, the positron momentum, or its mass. Because of the smallness of (l/M) these terms are negligible for all practical purposes.

[12]For the exact evaluation of J_2^{λ}, see Behrends *et al.*, Ref. 10, Eq. (7b) *et seq.* The integral $\hat{J}_2^{\lambda}$ can be obtained by similar methods.

PHYSICAL REVIEW D VOLUME 6, NUMBER 9 1 NOVEMBER 1972

Bootstrap Model of Inclusive Reactions*

J. Finkelstein†‡ and R. D. Peccei
Institute of Theoretical Physics, Department of Physics, Stanford University, Stanford, California 94305

(Received 26 June 1972)

We study a model in which multiparticle processes are envisaged as ocurring via the formation of a fireball and a leading particle. We impose a bootstrap condition on the fireball decay distribution by demanding that it be the same, in its rest system, as the over-all distribution in the c.m. system. This leads us to a set of integral equations for both single-particle and multiparticle inclusive distributions. We examine these equations in the scaling limit, we show that the multiplicity of produced particles grows logarithmically with energy and that the multiparticle distributions factorize for particles traveling in opposite directions, and we obtain a bound on the size of the two-particle distribution function. If Regge constraints are imposed, we show that the model predicts that the scaling limit for the single-particle distribution function, in the central region, is approached from below. Furthermore, many of the features of a Mueller analysis are clearly exhibited by the model. We illustrate various properties of the model by means of two examples, one of which is in qualitative agreement with experiment.

I. INTRODUCTION

Particle production is the dominant feature of high-energy collision processes, accounting for roughly 80% of all events, and a variety of models have been proposed to describe these processes.[1] Several of these models[2] consider high-energy processes occurring through the formation of one or several clusters of particles, often called fireballs, which then decay into the observed particles. A general assumption made in most of these models is that the decay of the fireball is isotropic in its own rest system; other details of the decay mechanism are part of the theoretical input which distinguishes among various versions of these models. In this paper we shall also envisage particle production processes as occurring via the formation of a fireball, but shall consider the alternative assumption that the fireball decay distribution, rather than being isotropic, is essentially the same as the distribution of particles in the entire event. This constitutes in effect a bootstrap hypothesis.

We shall imagine, for simplicity, a world of only

one kind of (scalar) particle of mass m. Toward the end of the paper we shall indicate what features can be extrapolated from this simple model so as to apply to actual data, and how the idea itself can be extended to a more realistic situation. Our focus will be on inclusive distributions, since these provide an alternate, and in our model simpler, way of describing multiparticle processes than exclusive distributions.

For any given event, we concentrate our attention on a single produced particle, which we refer to as the leading particle,[3] and on the distribution of the rest, which we refer to collectively as the fireball. The hypothesis which we shall make is that the inclusive distribution resulting from the fireball decay, as seen in its own rest system, is the same as the total inclusive distribution in the overall c.m. system save for the fact that what plays the role of s (the square of the total energy in the c.m. system) for the fireball decay is the fireball total invariant mass squared, M^2. This bootstrap hypothesis is essentially identical to the one proposed by Krzywicki and Petersson[4] but has been arrived at independently. It is clear that a simple multiperipheral model in which the exchanged object is the same as the produced particle can satisfy this hypothesis when the "leading" particle is identified with the particle appearing at the end of the multiperipheral chain. However, the model we discuss is more general than this, a fact that will become clearer, for example, when we examine the Regge content of the model in the pionization region. Our model is also similar in spirit to a statistical model, in that we assume that the fireball is itself composed of a leading particle and a fireball.[5] Our basic assumption is that the distribution of particles is sufficiently chaotic so that, when one subtracts out the leading particle, the same chaos remains.[6]

The plan of the paper is as follows: In Sec. II, and in an appendix, we derive the basic equations of the model and study these equations in the scaling limit, deducing various general properties of the model. We show that knowledge of the leading-particle distribution determines uniquely both the single-particle and the many-particle inclusive distributions. Furthermore we show that the many-particle inclusive distributions exhibit factorization properties that arise from absence of correlations among particles traveling in opposite directions. We obtain restrictions on the possible shape of the single-particle spectrum and obtain an upper bound on the two-particle correlation function in the central region. We also verify that all energy-momentum constraints are satisfied by the bootstrap model. In Sec. III we examine the consequences of imposing Regge constraints on the single-particle distribution at $x=0$ and $x=\pm 1$. The most interesting consequence of imposing these constraints is that the single-particle distribution at $x=0$ approaches the scaling limit from *below*, as the energy increases, in accord with the recent ISR (CERN Intersecting Storage Rings) data.[7] Other consequences that follow from these restrictions on the model are that there exists a finite correlation length determined, as expected, in terms of the intercept of the secondary Regge trajectory, and that the two-particle correlation function is positive (at least for large rapidity separation in the central region). Section IV is devoted to illustrating some features of the model by two specific choices of the leading-particle distribution, one of which yields flat inclusive distributions and the complete absence of dynamical correlations, and the other which gives results in qualitative agreement with experiment. In the last section, Sec. V, we summarize some of the salient features of the model and suggest possible ways to render the model more realistic.

II. GENERAL THEORY

We consider a world of one type of scalar particle. We shall define the single-particle inclusive distribution, at total c.m. energy squared s, as

$$N(\vec{p}, s) = \frac{1}{\sigma_{\text{tot}}} \frac{d\sigma}{dp}, \quad dp = \frac{d^3p}{E} \tag{1}$$

so that

$$\int dp N(\vec{p}, s) = \langle n(s) \rangle . \tag{2}$$

In each event we distinguish one particle, which we call the leading particle, with a distribution $N_L(\vec{p}, s)$, and refer to the rest of the other particles as the fireball. Since there is one leading particle per event it follows that

$$\int dp N_L(\vec{p}, s) = 1 . \tag{3}$$

Consider now a produced particle of momentum $\vec{p}$. Two possibilities exist: Either it is a leading particle, of momentum $\vec{p}$, or it comes from the fireball. In this latter case the leading particle has some other momentum, say $\vec{p}'$. Let us denote by N_F the decay distribution of the fireball. Then we can write

$$N(\vec{p}, s) = N_L(\vec{p}, s) + \int dp' N_L(\vec{p}', s) N_F((\Lambda_{p'}\vec{p}), M^2) . \tag{4}$$

We have written the arguments of N_F in the fireball rest frame, so that $\Lambda_{p'}$ is the Lorentz transformation that takes us from the c.m. frame to the fire-

ball frame (we use $\Lambda_{p'}\vec{p}$ to denote the three-vector after the transformation), and M^2 is the invariant mass squared of the fireball, which of course depends on $\vec{p}'$, the momentum against which the fireball recoils. Except for the fact that we have not displayed the possible dependence of N_F on $\vec{p}'$ and on s, Eq. (4) is general and merely expresses mathematically the two possibilities mentioned above. The bootstrap hypothesis we shall adopt is that N_F is the same function of its arguments as is N. Equation (4) is then essentially the same "recursion relation" for N obtained by Krzywicki and Petersson.[4]

To proceed further, we shall now assume that $N_L(\vec{p}, s)$ has a scaling limit,[8] and that all transverse momenta are limited. We define

$$x = 2p_{\parallel}/\sqrt{s}\ , \quad y = 2p'_{\parallel}/\sqrt{s}\ , \quad z = 2(\Lambda_{p'}\vec{p})_{\parallel}/M. \tag{5}$$

In the scaling limit it is easy to check that[9]

$$dp' = \frac{dy}{|y|}\, d^2p'_{\perp}\ ,$$

$$z = \begin{cases} x & \text{if } xy<0 \\ \dfrac{x}{1-|y|} & \text{if } xy>0, \end{cases} \tag{6}$$

$$(\Lambda_{p'}\vec{p})_{\perp} = \vec{p}_{\perp} + \vec{k}_{\perp}(x, y, \vec{p}'_{\perp}),$$

where

$$\vec{k}_{\perp}(x, y, \vec{p}'_{\perp}) = \begin{cases} (x/y)[(1-|y|)^{1/2} - 1]\,\vec{p}'_{\perp} & \text{if } xy<0 \\ (x/y)\left[\dfrac{1}{(1-|y|)^{1/2}} - 1\right]\vec{p}'_{\perp} & \text{if } xy>0. \end{cases}$$

If we pick, for definitiveness, $x \geq 0$, then Eq. (4) becomes

$$N(x, \vec{p}_{\perp}) = N_L(x, \vec{p}_{\perp}) + \int d^2p'_{\perp}\left[\int_{-1}^{0} \frac{dy}{|y|}\, N_L(y, \vec{p}'_{\perp}) N(x, \vec{p}_{\perp} + \vec{k}_{\perp}) + \int_0^1 \frac{dy}{y}\, N_L(y, \vec{p}'_{\perp}) N\left(\frac{x}{1-y}, \vec{p}_{\perp} + \vec{k}_{\perp}\right)\right] \quad (x \geq 0). \tag{7}$$

The above equation is an integral equation for N, once N_L is given. For the rest of this paper we shall consider only the simpler equation obtained by integrating Eq. (7) over transverse momenta. Defining

$$f(x) = \int d^2p_{\perp}\, N(x, \vec{p}_{\perp}),$$

$$g(x) = 2\int d^2p_{\perp}\, N_L(x, \vec{p}_{\perp}), \tag{8}$$

we have

$$f(x) = \tfrac{1}{2} g(x) + \tfrac{1}{2}\int_{-1}^{0} \frac{dy}{|y|}\, g(y) f(x) + \tfrac{1}{2}\int_0^1 \frac{dy}{y}\, g(y) f\left(\frac{x}{1-y}\right) \qquad (x \geq 0). \tag{9}$$

Recalling that $N_L(y, \vec{p}'_{\perp})$ was normalized to unity [Eq. (3)], and using the fact that the distribution is symmetric in y, we have that

$$\int_0^1 \frac{dy}{y}\, g(y) = 1. \tag{10}$$

Hence we can immediately rewrite Eq. (9) as

$$f(x) = g(x) + \int_0^{1-x} \frac{dy}{y}\, g(y) f\left(\frac{x}{1-y}\right) \quad (x \geq 0). \tag{11}$$

The upper limit in Eq. (11) is $1-x$ because kinematically f is zero when its argument exceeds 1. Equation (11) has also been obtained in Ref. 4.

The solution to Eq. (11) satisfies automatically the inclusive sum rules that follow from energy-momentum conservation.[10] These sum rules are obviously satisfied by N as given in Eq. (4) provided that N_F itself satisfies them. However, it is perhaps not so clear that once the bootstrap hypothesis is made, no solution violating energy-momentum exists for Eq. (11). To see that this is the case we integrate Eq. (11) over x. Then we have

$$\int_0^1 dx\, f(x) = \int_0^1 dx\, g(x) + \int d\left(\frac{x}{1-y}\right)\int \frac{dy}{y}\, g(y)(1-y) f\left(\frac{x}{1-y}\right)$$

$$= \int_0^1 dx\, g(x) + \int_0^1 dx\, f(x)\left(1 - \int_0^1 dy\, g(y)\right), \tag{12}$$

implying

$$\int_0^1 dx\, f(x) = 1, \tag{13}$$

which is precisely the energy sum rule. The momentum sum rule is trivial because f is symmetric in x.

Equation (11) is a Volterra equation for f in terms of g, with a possible weak singularity since $g(x)/x$ need not be bounded when $x \to 0$. It can be solved by taking Mellin transforms. If we define

$$h(x) = x\frac{g(1-x)}{1-x} \tag{14}$$

the integral in Eq. (11) is the Mellin convolution of f with h. Denoting the Mellin transform of f by

$$\hat{f}(\lambda)=\int_0^1 dx\, x^{\lambda-1} f(x), \tag{15}$$

we have

$$\hat{f}(\lambda)=\frac{\hat{g}(\lambda)}{1-\hat{h}(\lambda)}. \tag{16}$$

Upon inversion, Eq. (16) gives the solution of the integral equation.

Given a g, or equivalently a leading-particle distribution, one has a unique solution for f. It follows directly also, from the Volterra nature of the integral equation, that

$$f(x)\geq g(x), \tag{17}$$

since the iterative solution of Eq. (11) converges and is positive since g is. We could equally well regard Eq. (11) as an equation for g given f. However, as we shall see below, not all functions $f(x)$ will guarantee that the resultant $g(x)$ is positive. Hence Eq. (11) determines an acceptable $f(x)$ in terms of $g(x)$, the converse not being necessarily the case.

It is clear from Eqs. (10) and (14) that $\hat{g}(0)=\hat{h}(0)=1$. Furthermore, since $g(x)$ and consequently $h(x)$ are positive, it follows that for $\mathrm{Re}\lambda>0$ both $\hat{g}(\lambda)$ and $\hat{h}(\lambda)$ are in magnitude less than unity and are analytic there. Thus $\hat{f}(\lambda)$ has as its leading singularity a pole at $\lambda=0$ which implies that $f(x=0)=$ constant. The value of this constant is just the residue of the pole of $\hat{f}(\lambda)$ at $\lambda=0$:[11]

$$f(0)=\left[-\frac{d}{d\lambda}\hat{h}(\lambda)\Big|_{\lambda=0}\right]^{-1}$$

$$=\left[-\int_0^1\frac{dx}{x}\,g(x)\ln(1-x)\right]^{-1}. \tag{18}$$

Since $f(0)$ is finite it follows that, as expected, the particle multiplicity increases logarithmically with energy,

$$\langle n(s)\rangle = f(0)\ln s \quad (s\to\infty). \tag{19}$$

We may use the result of Eq. (18) along with the fact that $f(x)\geq g(x)$ to deduce a general restriction on $f(x)$, namely,

$$f(0)\geq\left[-\int_0^1\frac{dx}{x}f(x)\ln(1-x)\right]^{-1}. \tag{20}$$

This is an example of the restrictions on f that follows from positivity of g. What this restriction roughly says is that if $f(x)$ has a hole near $x=0$, it cannot be too deep, otherwise it cannot be a solution of Eq. (11). If one uses the energy-momentum sum rule, Eq. (13), it is easy to see that Eq. (20) is always satisfied if $f(0)\geq 1$.

Having discussed some of the general properties of the equation for the single-particle inclusive distribution, let us now turn to the equations that describe the many-particle inclusive distributions. We shall consider these equations only in the scaling limit and shall integrate over transverse momenta. We begin by defining an n-particle inclusive distribution as

$$f_n(x_1,\ldots,x_n)=\frac{1}{\sigma_{\mathrm{tot}}}(|x_1|\cdots|x_n|)\frac{d\sigma}{dx_1\cdots dx_n}. \tag{21}$$

In this notation f_1 is what we have previously called f. We should note that if more than one of the arguments of f_n vanishes then f_n is not uniquely determined. However, it will be interesting to consider the limits of f_n as its arguments approach zero in various ways.

We can now proceed to derive an integral equation for f_n in much the same way as we derived the equation for f_1. Suppose there are produced particles at $x_1, x_2, \ldots, x_n$. Again there are two possibilities: Either the leading particle is at x_i (some $i\leq n$), in which case the fireball provides the other $n-1$ particles, or the leading particle is at some other value y and the fireball provides all the n particles. The bootstrap hypothesis which we adopt is that the n and $(n-1)$-particle distributions from the fireball are given by f_n and f_{n-1}, respectively. Thus we have

$$f_n(x_1,\ldots,x_n)=\tfrac{1}{2}\sum_{i=1}^{n} g(x_i) f_{n-1}(z(x_1,x_i),\ldots,z(x_{i-1},x_i),z(x_{i+1},x_i),\ldots,z(x_n,x_i))$$

$$+\tfrac{1}{2}\int_{-1}^{1}\frac{dy}{|y|}\,g(y) f_n(z(x_1,y),\ldots,z(x_n,y)) \qquad (n\geq 2), \tag{22}$$

where [recall Eq. (6)]

$$z(a,b)=\begin{cases} a & \text{if } ab<0 \\ \dfrac{a}{1-|b|} & \text{if } ab>0 \end{cases} \tag{23}$$

and the factor of $\frac{1}{2}$ come from the factor of 2 in the definition of g, Eq. (8). If we know g and f_{n-1}, Eq. (22) is an integral equation for f_n. In the Appendix we show how this equation may be solved by taking Mellin transforms. Thus we see that knowing g we can obtain $f\equiv f_1$ from Eq. (11) and then obtain $f_2, f_3, \ldots, f_n$ from Eq. (22). Alternatively, if we

know f_1, and if Eq. (11) has a unique non-negative solution for g, we may eliminate g altogether from Eq. (22) and obtain all f_n, $n \geq 2$, in terms of f_1, the single-particle distribution.

The multiparticle integral equation, Eq. (22), possesses factorization properties. These matters are considered in detail in the Appendix, where we show that there are no correlations between particles traveling in opposite directions. That is, if $x_1 \cdots x_k < 0$ and $x_{k+1} \cdots x_n > 0$, then

$$f_n(x_1, \ldots, x_k, x_{k+1}, \ldots, x_n) = f_k(x_1, \ldots, x_k) f_{n-k}(x_{k+1}, \ldots, x_n). \tag{24}$$

In the Appendix we also show that the functions f_n obey the sum rules that follow from energy-momentum conservation.[10]

For the two-particle distribution, we then need only consider $f_2(x_1, x_2)$ when $x_1, x_2 > 0$. Let $x_2 = Rx_1$; as $s \to \infty$, R is related to the rapidity difference $y_2 - y_1$ by

$$y_2 - y_1 = \ln R + \ln \frac{m_{\perp 1}}{m_{\perp 2}} = \ln R \quad (R \to 0), \tag{25}$$

where $m_{\perp i}$ is the transverse mass, $m_{\perp i} = (m^2 + \vec{p}_{\perp i}^{\,2})^{1/2}$. If we define

$$f_2^R(x) = f_2(x, Rx) \tag{26}$$

then it follows from Eq. (22) that $f_2^R(x)$ satisfies [see also Eq. (A7)]

$$f_2^R(x) = g(x) f\left(\frac{Rx}{1-x}\right) + g(Rx) f\left(\frac{x}{1-Rx}\right) + \int_0^{1-x} \frac{dy}{y} g(y) f_2^R\left(\frac{x}{1-y}\right). \tag{27}$$

It is clear from the above that $f_2^R(x)$ vanishes for $x > 1/(1+R)$ as it must from energy-momentum conservation.

We see that $f_2^R(x)$ satisfies the same integral equation which f does, except that the inhomogeneous term is changed. Denoting this inhomogeneous term by $G_2^R(x)$ we obtain the Mellin transform solution of Eq. (27) as

$$\hat{f}_2^R(\lambda) = \frac{\hat{G}_2^R(\lambda)}{1 - \hat{h}(\lambda)}. \tag{28}$$

It is of special interest to study $f_2^R(x=0)$, since this puts us in the central region for the two-particle distribution with a finite rapidity separation, characterized by R. Now $f_2^R(0)$ is just the residue of the pole at $\lambda = 0$ in Eq. (28), so we have

$$\begin{aligned} f_2^R(0) &= \left[-\frac{d}{d\lambda} \hat{h}(\lambda) \Big|_{\lambda=0} \right]^{-1} \hat{G}_R(0) \\ &= f(0) \hat{G}_R(0) \\ &= f(0) \int_0^{(1+R)^{-1}} \frac{dx}{x} \left[g(x) f\left(\frac{Rx}{1-x}\right) + g(Rx) f\left(\frac{x}{1-Rx}\right) \right]. \end{aligned} \tag{29}$$

We may use Eq. (29) to bound $f_2^R(0)$, for if $f_{\max}$ is the maximum value attained by f we have

$$f_2^R(0) \leq f(0) f_{\max} \int_0^{(1+R)^{-1}} \frac{dx}{x} [g(x) + g(Rx)], \tag{30}$$

which on using Eq. (10) becomes

$$f_2^R(0) \leq 2 f(0) f_{\max}. \tag{31}$$

Since, experimentally, it appears that $f(x)$ attains its maximum at $x = 0$, we have

$$f_2^R(0) \leq 2[f(0)]^2. \tag{32}$$

The above implies that, in the central region and in the scaling limit, the two-particle correlation function satisfies

$$C_2(x_1, x_2) \equiv f_2(x_1, x_2) - f(x_1) f(x_2) \leq [f(0)]^2 \quad (x_1, x_2 \to 0). \tag{33}$$

III. REGGE CONSTRAINTS

Up to now we have studied some general properties of the bootstrap equations. We wish, in this section, to inject some information that comes from a Regge analysis of inclusive reactions.[12] According to Regge theory, the shape of the limiting distribution $f(x)$, near $x = \pm 1$ and $x = 0$, is governed respectively by the triple-Regge and pionization Mueller diagrams shown in Fig. 1. We shall impose this Regge behavior on $f(x)$ as a constraint on the model.

The triple-Regge diagram of Fig. 1(a) corresponds to the production of a fireball through the exchange of a Regge trajectory of intercept α_1. This yields a behavior of $f(x)$, near $x = \pm 1$, which is given by

$$f(x) \sim (1 - |x|)^{1-2\alpha_1} \quad (x \to \pm 1), \tag{34}$$

neglecting logarithmic terms.

The behavior of $f(x)$ as $x \to 0$ is given by the pionization diagram of Fig. 1(b). The exchange of the Pomeranchukon together with a trajectory of intercept α_0 yields, as shown by Brower and Ellis,[13]

$$f(x) \sim |x|^{1-\alpha_0} \quad (x \to 0). \tag{35}$$

With $\alpha_0 = \alpha_P = 1$ we obtain the constant $f(0)$. The high-lying trajectories that will appear in Eq. (35)

have, except for the Pomeranchukon, an approximately common intercept $\alpha_0 \simeq \frac{1}{2}$. Separating the Pomeranchukon term, we expect then

$$f(x) = f(0) + A\,|x|^{1-\alpha_0} \quad (x \to 0), \tag{36}$$

where A is a constant to be determined.

Up to now we have considered the bootstrap equations as being a bootstrap for the entire process. While there is not *a priori* any reason why diffractive processes, if they survive at infinite energies, should not bootstrap along with everything else, we here shall investigate a different possibility, namely, that the bootstrap we are describing is only for the nondiffractive part.[14] That is, the fireball decay distribution is taken to be the same as the nondiffractive part of the over-all process. In a multiperipheral model this would correspond to not including the Pomeranchuk trajectory in the input of the multiperipheral calculation. Technically this means that, in Eq. (34), α_1 is never taken to be $\alpha_P = 1$. With $\alpha_1 \simeq \frac{1}{2}$, $f(x)$ is approximately constant as $x \to \pm 1$. The results obtained below for the behavior of $f(x)$ near $x = 0$ depend on not including diffraction within the bootstrap.

With this limited bootstrap hypothesis, it should be clear that, if diffraction does persist at infinite energy, we must modify our definitions of f and f_n in Eqs. (1) and (21) by replacing σ_{tot} by the nondiffractive cross section. Furthermore, our results below, which show that correlations in this model are of short range, should also be understood as being due to our lack of inclusion of diffractive processes since, as is well known,[15] nonvanishing diffractive processes lead to long-range correlations.

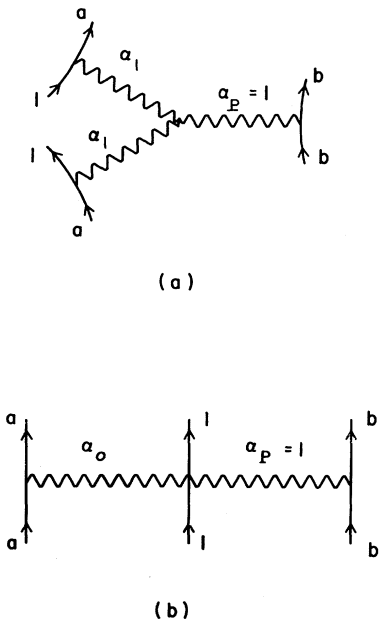

FIG. 1. (a) Triple-Regge diagram for the process $a + b \to 1 +$ anything which determines the shape of $f(x)$ as $x \to \pm 1$. (b) Pionization diagram for the process $a + b \to 1 +$ anything which determines the shape of $f(x)$ as $x \to 0$.

The λ plane used to solve Eq. (11) by Mellin transforms can be identified as an angular momentum plane. A pole in $\hat{f}(\lambda)$ at $\lambda = \lambda_0$ corresponds to a behavior of $f(x)$, near $x = 0$, like $|x|^{-\lambda_0}$. We have seen in Eq. (35) that such a behavior corresponds to a Regge pole with intercept $\alpha_0 = \lambda_0 + 1$.

The leading singularities of $\hat{f}(\lambda)$ are poles at $\lambda = 0$ (which we have discussed previously) and at $\lambda = \alpha_0 - 1 \simeq -\frac{1}{2}$. A pole in $\hat{f}(\lambda)$ can arise either from a pole in $\hat{g}(\lambda)$ or from a zero in the denominator when $\hat{h}(\lambda) = 1$. $\hat{h}(\lambda)$ is given by

$$\hat{h}(\lambda) = \int_0^1 dx\, x^{\lambda} \frac{g(1-x)}{1-x}\,. \tag{37}$$

The convergence of the above integral is determined by the behavior of $g(x)$ as $x \to 1$. Since $g(x) \leq f(x)$, using Eq. (34), we see that the integral defining $\hat{h}(\lambda)$ converges for $\mathrm{Re}\lambda > -2 + 2\alpha_1$. Since $h(x)$ is positive, $\hat{h}(\lambda)$ is monotonically decreasing for $\mathrm{Re}\lambda > -2 + 2\alpha_1$. Furthermore, $\hat{h}(0) = 1$, so that $\hat{h}(\alpha_0 - 1 \simeq -\frac{1}{2}) > 1$ provided that $-2 + 2\alpha_1 < \alpha_0 - 1$. This last inequality is satisfied if the trajectory exchanged in the triple-Regge limit is an ordinary trajectory, for then $\alpha_1 \simeq \alpha_0 \simeq \frac{1}{2}$. In this case, then, the pole at $\lambda = \alpha_0 - 1$ in $\hat{f}(\lambda)$ must come directly from a pole in $\hat{g}(\lambda)$ at $\lambda = \alpha_0 - 1$, so that we can write

$$g(x) = B\,|x|^{1-\alpha_0} \quad (x \to 0). \tag{38}$$

The coefficient of $|x|^{1-\alpha_0}$ in Eq. (36) is then

$$A = \frac{B}{1 - \hat{h}(\alpha_0 - 1)}\,. \tag{39}$$

The value of A of course depends on what is the precise form of g. However, the sign of A does not: Since $g(x)$ is positive we have $B > 0$; since $\hat{h}(\alpha_0 - 1) > 1$ it follows that $A < 0$. This means that $f(x)$ has an (at least local) maximum at $x = 0$.

The Mueller diagram of Fig. 1(b) also gives the approach to scaling in the central region. In terms of the parametrization used in Eq. (36) one has

$$\int d^2p_\perp \frac{d\sigma}{dp}(p_\parallel = 0, s) = f(0) + \frac{2A}{(s^{1/2}/m_\perp)^{1-\alpha_0}}\,. \tag{40}$$

Since $A < 0$, the distribution is predicted by the bootstrap model to approach the scaling limit from below, in agreement with the recent ISR data.[7] We should remark that most other models, including the multiperipheral model,[16] obtain an incorrect

sign for A.

In general, it is possible for zeros in the denominator in Eq. (16) to produce poles in $\hat{f}(\lambda)$ at complex values of λ, as well as at real values for $\mathrm{Re}\lambda < -2+2\alpha_1$. However, if $g(x)/x$ is a monotonically decreasing function of x, as is true in the examples discussed in the next section, then this cannot happen for $\mathrm{Re}\lambda > -2+2\alpha_1$ since $\mathrm{Im}\hat{h}(\lambda)$ does not vanish there.

We have seen in the previous section that there are no correlations between particles traveling in opposite directions. The Mueller diagram shown in Fig. 2 gives, by a now-standard analysis,[17] a short-range correlation in the central region with correlation length $\xi = (1-\alpha_0)^{-1}$. That such a behavior follows in the model can be seen directly from Eq. (29). Expanding f and g according to Eqs. (36) and (38) we have, as $R \to 0$,

$$f_2^R(0) = f(0)\left\{\int_0^1 \frac{dx}{x}\, g(x)\left[f(0) + AR^{1-\alpha_0}\left(\frac{x}{1-x}\right)^{1-\alpha_0}\right] + BR^{1-\alpha_0}\int_0^1 \frac{dx}{x} f(x)x^{1-\alpha_0}\right\}. \tag{41}$$

The two-particle correlation function in the central region is given by

$$C_2^R(0) \equiv f_2^R(0) - [f(0)]^2$$
$$= R^{1-\alpha_0}\left[A\int_0^1 \frac{dx}{x}\, g(x)\left(\frac{x}{1-x}\right)^{1-\alpha_0} + B\int_0^1 \frac{dx}{x} f(x)x^{1-\alpha_0}\right] \quad (R \to 0). \tag{42}$$

Since, for small R, $R = e^{y_2 - y_1}$, we indeed have a correlation length given by $\xi = (1-\alpha_0)^{-1}$. Similarly, it can be shown that the many-particle correlation functions all disappear with a correlation length ξ as $R \to 0$. The value of the coefficient of $R^{1-\alpha_0}$ in Eq. (42) depends explicitly on what g is; however, it is not hard to show that the coefficient itself is positive, for any choice of g.[18]

IV. EXAMPLES

A very simple example can be obtained by choosing $g(x) = x$. This example, of course, does not obey the Regge constraints discussed in the previous section, but it is nevertheless amusing to consider it. We should note that this example has also been discussed in Ref. 4.

With this choice of $g(x)$ one has that

$$\hat{g}(\lambda) = \hat{h}(\lambda) = (1+\lambda)^{-1}. \tag{43}$$

Then from Eq. (16) it follows that $\hat{f}(\lambda) = \lambda^{-1}$, which implies $f(x) = 1$. In fact it is easy to show that for any n, $f_n(x_1, \ldots, x_n) = 1$ whenever it is kinematically allowed to exist. This means that, in this example, there are no correlations whatsoever.

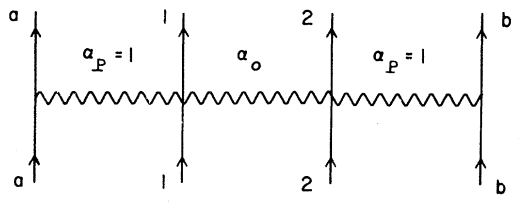

FIG. 2. Mueller diagram for $a + b \to 1 + 2 +$ anything which gives rise to a correlation of range $\xi = (1-\alpha_0)^{-1}$.

For a more realistic example, we can impose the Regge constraints of the previous section. For simplicity we shall take $\alpha_0 = \alpha_1 = \frac{1}{2}$. Then $g(x) \sim x^{1/2}$ as $x \to 0$ and $g(x) \to$ constant as $x \to 1$. The simplest function compatible with these constraints is

$$g(x) = \tfrac{1}{2}x^{1/2}, \tag{44}$$

and we adopt this choice of $g(x)$ for our second example. In fact, it can be argued that this form for g is not totally unrealistic. In proton-proton scattering most of the produced particles are pions, except near $x = \pm 1$, but in a large fraction of the events the two protons are the leading particles. Except for small x, what we are calling the leading-particle spectrum should be rather similar to the actual spectrum of leading particles, the protons in pp collisions.

In Fig. 3 we display the function $g(x) = \frac{1}{2}x^{1/2}$, together with points representing the proton spectrum integrated over $p_\perp$ at $P_{\mathrm{lab}} = 19.2$ GeV/c, which perhaps is sufficiently close to the scaling limit. The data are from Ref. 19, and the errors arise mostly from our uncertainty in integrating over $p_\perp$. Our choice of $g(x)$ does seem to qualitatively fit the data, although we must reiterate that there is no reason to suppose that near $x = 0$ $g(x)$ has anything to do with the proton spectrum.

We have displayed in Fig. 4 the function $f(x)$, along with $g(x)$, obtained by numerically solving Eq. (11) with $g(x)$ given by Eq. (44). This function is supposed to represent, in the scaling limit, the combined inclusive distribution of all produced particles. Its value at $x = 0$ is 1.63, which implies $\langle n(s)\rangle = 1.63 \ln s$. This number is slightly larger than would be expected from the Echo Lake data,[20]

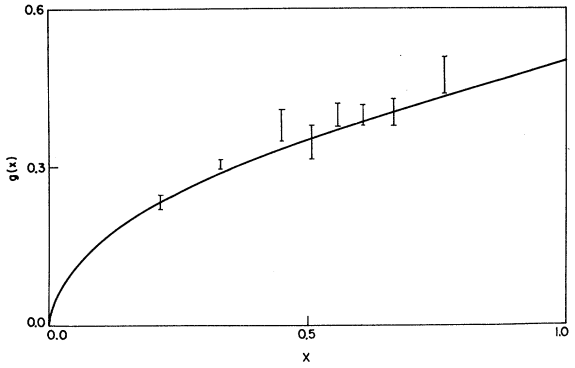

FIG. 3. The function $g(x) = \frac{1}{2}x^{1/2}$ together with experimental points for the process $p + p \to p +$ anything from Ref. 19, plotted against x.

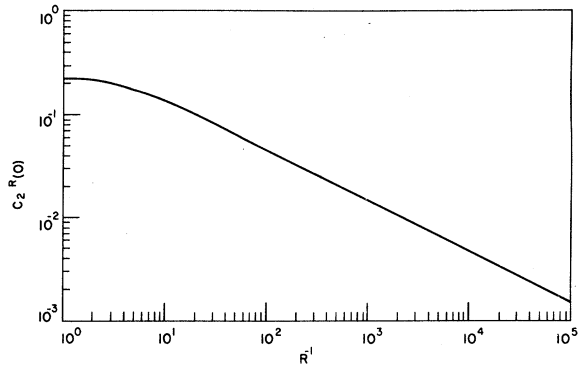

FIG. 5. The two-particle correlation function in the central region $C_2^R(0)$ plotted against R^{-1}.

but more recent ISR data[7] indicate that this number should be higher. The value of A obtained, Eq. (39), is $A = -0.87$, which on taking $\langle m_\perp \rangle = 0.4$ GeV predicts

$$\frac{1}{\sigma_{\text{tot}}}\left(|x|\frac{d\sigma}{dx}\right)_{x=0} = 1.63\left(1 - \frac{0.68}{s^{1/4}}\right), \tag{45}$$

with s measured in GeV^2. If Eq. (40) were valid down to conventional accelerator energies, which is not at all certain, then a comparison of data at these energies[21] with ISR data would indicate that the value of A should be perhaps 2.5 times as large as the value given here.

The sharp rise in $f(x)$ near $x = 1$ occurs because of the assumed behavior of $g(x) \sim x^{1/2}$, which implies that near $x = 1$ the integral in Eq. (11) behaves as $(1-x)^{1/2}$. In general any behavior of $g(x)$ near $x = 0$ as $Bx^{1-\alpha_0}$ will yield a contribution to $f(x)$ near $x = 1$ of the form $(1-x)^{1-\alpha_0}$ from the integral. It might be amusing to interpret this behavior of $f(x)$ as being due to K^* exchange with $\alpha_{K^*}(0) \simeq \frac{1}{4}$. However, in general the inhomogeneous term in Eq. (11) could contain terms that cancel this behavior.

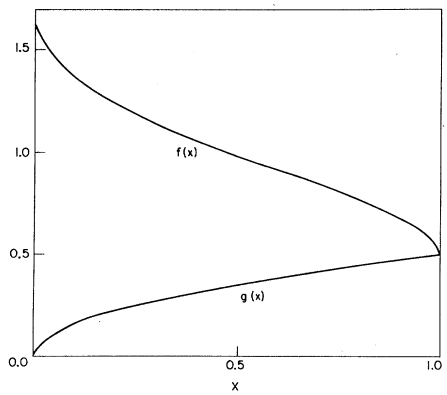

FIG. 4. The function $g(x) = \frac{1}{2}x^{1/2}$ and the resultant function $f(x)$, obtained by solving Eq. (11), plotted against x.

Having obtained the single-particle distribution, in this example, we have also calculated the two-particle correlation function in the central region. The result is displayed in Fig. 5. As can be seen the correlation is not large; the maximum value of $C_2^R(0)$ is about 10% of $[f(0)]^2$, which easily satisfies the bound of Eq. (32). The value of the coefficient of $R^{1/2}$ in Eq. (42) is 0.475.

In the absence of any long-range correlations, the integrated two-particle correlation behaves, at large energy, as

$$\langle C_2 \rangle = C \ln s \quad (s \to \infty), \tag{46}$$

with

$$C = 2\int_0^1 \frac{dR}{R} C_2^R(0). \tag{47}$$

In our example, we find $C = 0.9 f(0)$. This provides a measure of the deviation of the exclusive n-particle cross-section distributions from a Poisson distribution, since

$$\frac{\langle (n - \langle n \rangle)^2 \rangle}{\langle n \rangle} = 1 + \frac{\langle C_2 \rangle}{\langle n \rangle} = 1 + \frac{C}{f(0)} \quad (s \to \infty). \tag{48}$$

V. CONCLUDING REMARKS

We have discussed a bootstrap model of inclusive reactions in a world of one type of particle. The model is solvable for all n-particle inclusive distribution functions once the input leading-particle distribution is given. It presents various attractive features: For example, it automatically satisfies energy-momentum constraints, it predicts

factorization among particles which travel in opposite directions, and is amenable to the inclusion of Regge constraints. The main difficulty of the model, at this stage, is including (or excluding) diffractive processes in a natural way.

It is clear that the model can be improved in at least two ways. The first is by improving our guess for $g(x)$ so as to obtain, perhaps, more realistic results. For example, increasing the value of B in Eq. (38) would tend to increase the value of $f(0)$. The second and more necessary step would be to introduce quantum numbers into the model. This would lead naturally to systems of coupled integral equations for distributions f^i with various unknown leading-particle distributions, g^i. An attractive idea would be to use experimental data to obtain the various f^i, solve the integral equations to obtain the g^i, and then use these in conjunction with the input f^i to obtain the two-particle distribution functions predicted by the model and compare these distributions with experiment.

We have, in this paper, concentrated on the bootstrap equations integrated over transverse momenta and evaluated in the scaling limit. However, these equations might also be used to discuss a bootstrap of the $p_\perp$ dependence, and/or to study the approach to scaling.

Finally, we should remark on a purely theoretical virtue of the model. It contains, in a very simple but hopefully clear fashion, many features of the multiperipheral model, of the statistical picture, and of Mueller's approach to inclusive reactions.

APPENDIX

In this appendix we shall show how to solve Eq. (22) by use of Mellin transforms, and prove that the solution exhibits the factorization property Eq. (24) and that it obeys the energy-momentum sum rules.

Suppose, for definitiveness, that $x_i < 0$ $(i \leq k)$, $x_i > 0$ $(i > k)$. Then we shall write

$$x_i = L_i x_1 \quad (L_1 = 1;\ i \leq k),$$
$$x_i = R_i x_n \quad (R_n = 1;\ k < i \leq n), \tag{A1}$$

and

$$f_n(x_1, \ldots, x_k, x_{k+1}, \ldots, x_n) \equiv f_n(L_1 x_1, \ldots, L_k x_1, R_{k+1} x_n, \ldots, R_n x_n)$$
$$\equiv f^{L,R}_{k,n-k}(x_1, x_n), \tag{A2}$$

with the convention

$$f^{L,R}_{0,n}(x_1, x_n) = f^R_n(x_n), \qquad f^{L,R}_{n,0}(x_1, x_n) = f^L_n(x_1).$$

In terms of this notation we can write Eq. (22) as

$$f^{L,R}_{k,n-k}(x_1, x_n) = \tfrac{1}{2} G^{L,R}_{k,n-k}(x_1, x_n) + \tfrac{1}{2}\int_{-1}^{0} \frac{dy}{|y|} g(y) f^{L,R}_{k,n-k}\left(\frac{x_1}{1-|y|}, x_n\right) + \tfrac{1}{2}\int_0^1 \frac{dy}{y} g(y) f^{L,R}_{k,n-k}\left(x_1, \frac{x_n}{1-y}\right), \tag{A3}$$

where, for $0 \neq k \neq n$,

$$G^{L,R}_{k,n-k}(x_1, x_n) = \sum_{i=1}^{k} g(L_i x_1) f^{L,R}_{k-1,n-k}\left(\frac{x_1}{1-|L_i x_1|}, x_n\right) + \sum_{i=k+1}^{n} g(R_i x_n) f^{L,R}_{k,n-k-1}\left(x_1, \frac{x_n}{1-R_i x_n}\right). \tag{A4}$$

In the first (second) sum in Eq. (A4) f does not depend on L_i (R_i).

Consider first $0 \neq k \neq n$. We define the two-dimensional transform

$$\hat{f}^{L,R}_{k,n-k}(\lambda_1, \lambda_n) = \int_{-1}^{0} dx_1 x_1^{\lambda_1 - 1} \int_0^1 dx_n x_n^{\lambda_n - 1} f^{L,R}_{k,n-k}(x_1, x_n). \tag{A5}$$

It is easy to see that Eq. (A3) has the solution

$$\hat{f}^{L,R}_{k,n-k}(\lambda_1, \lambda_n) = \frac{\frac{1}{2}\hat{G}^{L,R}_{k,n-k}(\lambda_1, \lambda_n)}{1 - \frac{1}{2}[\hat{h}(\lambda_1) + \hat{h}(\lambda_n)]}. \tag{A6}$$

If $k = 0$, then Eq. (A3) simplifies to

$$f_n^R(x_n) = G_n^R(x_n) + \int_0^1 \frac{dy}{y}\, g(y) f_n^R\left(\frac{x_n}{1-y}\right), \tag{A7}$$

with

$$G_n^R(x_n) = \sum_{i=1}^{n} g(R_i x_n) f_{n-1}^R\left(\frac{x_n}{1-R_i x_n}\right), \tag{A8}$$

where in the sum f does not depend on R_i. In this case it is sufficient to define the one-dimensional transform

$$\hat{f}_n^R(\lambda_n) = \int_0^1 dx_n\, x_n^{\lambda_n - 1} f_n^R(x_n), \tag{A9}$$

and Eq. (A7) has the transform solution

$$\hat{f}_n^R(\lambda_n) = \frac{\hat{G}_n^R(\lambda_n)}{1-\hat{h}(\lambda_n)}. \tag{A10}$$

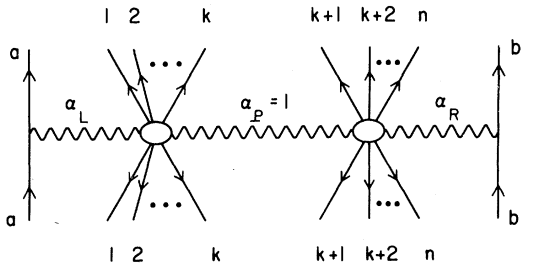

FIG. 6. Mueller diagram for the contribution to the process $a + b \to 1 + 2 + \cdots + n +$ anything of poles in $\hat{f}^{L,R}_{k,n-k}(\lambda_1, \lambda_n)$ at $\lambda_1 = \alpha_L - 1$, $\lambda_n = \alpha_R - 1$.

The case $k = n$ is treated similarly to the case $k = 0$.

We shall now prove that the transform solution (A6) possesses factorization properties, namely,

$$\hat{f}^{L,R}_{k,n-k}(\lambda_1, \lambda_n) = \hat{f}^L_k(\lambda_1)\hat{f}^R_{n-k}(\lambda_n). \tag{A11}$$

This equation is trivially satisfied if $k = 0$ or $k = n$ if we define $\hat{f}_0 = 1$. Equation (24) follows directly from Eq. (A11). What Eq. (A11) means in terms of a Regge picture is illustrated by the Mueller diagram of Fig. 6: Poles in (λ_1, λ_n) at $(\lambda_1^0, \lambda_n^0)$ correspond to trajectories with intercepts $(\alpha_L = \lambda_1^0 + 1,\ \alpha_R = \lambda_n^0 + 1)$.

For $n = 1$ Eq. (A11) is certainly true. Let us assume it for some $n-1$, and prove it for n. Under this inductive assumption, we can write

$$G^{L,R}_{k,n-k}(x_1, x_n) = G^L_k(x_1) f^R_{n-k}(x_n) + f^L_k(x_1)\, G^R_{n-k}(x_n) \tag{A12}$$

and

$$\hat{G}^{L,R}_{k,n-k}(\lambda_1, \lambda_n) = \hat{G}^L_k(\lambda_1)\hat{f}^R_{n-k}(\lambda_n) + \hat{f}^L_k(\lambda_1)\hat{G}^R_{n-k}(\lambda_n). \tag{A13}$$

From Eq. (A10) it follows that we can rewrite Eq. (A13) as

$$\tfrac{1}{2}\hat{G}^{L,R}_{k,n-k}(\lambda_1, \lambda_n) = \frac{\hat{G}^L_k(\lambda_1)}{1-\hat{h}(\lambda_1)} \frac{\hat{G}^R_{n-k}(\lambda_n)}{1-\hat{h}(\lambda_n)} \{1 - \tfrac{1}{2}[\hat{h}(\lambda_1) + \hat{h}(\lambda_n)]\}, \tag{A14}$$

and, using Eqs. (A6), (A10), and (A14), Eq. (A11) follows for arbitrary n.

Finally, we shall prove that the distributions f_n satisfy the energy-momentum sum rules.[10] Consider the case in which all $x_i > 0$; we shall prove that in this case

$$\int_0^1 dx_n\, f_n(x_1, \ldots, x_n) = \left(1 - \sum_{i=1}^{n-1} x_i\right) f_{n-1}(x_1, \ldots, x_{n-1}). \tag{A15}$$

With the convention $f_0 = 1$, Eq. (A15) has already been proven, for the case $n = 1$, in Eq. (13).

Now let us assume that Eq. (A15) is true for some $n-1$, and prove that it is true for n. Define

$$\bar{f}_n(x_1, \ldots, x_{n-1}) = \int_0^1 dx_n\, f_n(x_1, \ldots, x_n). \tag{A16}$$

Substituting in (A16) the expression for f_n in Eq. (22), we find

$$\bar{f}_n(x_1, \ldots, x_{n-1}) = \left(1 - \sum_{j=1}^{n-1} x_j\right) \sum_{i=1}^{n-1} g(x_i)\, f_{n-2}\left(\frac{x_1}{1-x_i}, \ldots, \frac{x_{i-1}}{1-x_i}, \frac{x_{i+1}}{1-x_i}, \ldots, \frac{x_n}{1-x_i}\right)$$

$$+ \int_0^1 dx_n\, g(x_n) f_{n-1}\left(\frac{x_1}{1-x_n}, \ldots, \frac{x_{n-1}}{1-x_n}\right) + \int_0^1 \frac{dy}{y}\, g(y)(1-y)\bar{f}_n\left(\frac{x_1}{1-y}, \ldots, \frac{x_{n-1}}{1-y}\right), \tag{A17}$$

where to get the first term on the right-hand side we have applied the inductive hypothesis to f_{n-1}. Consider Eq. (A17) as an integral equation for $\bar{f}_n$; it can be solved by taking a Mellin transform [compare the development that led to Eq. (A10)], and hence has a unique solution. But Eq. (A17) is solved by

$$\bar{f}_n(x_1, \ldots, x_{n-1}) = \left(1 - \sum_{i=1}^{n-1} x_i\right) f_{n-1}(x_1, \ldots, x_{n-1}), \tag{A18}$$

as can be seen by substituting Eq. (A18) into Eq. (A17) and making use of the integral equation [Eq. (22) or, equivalently, Eq. (A7)] satisfied by f_{n-1}. Equation (A18) is thus a correct expression for $\bar{f}_n$; this completes the proof of Eq. (A15) for arbitrary n.

We can now use Eq. (A15), together with the factorization property [Eq. (24)] to prove the energy and momentum sum rules. Let $x_i < 0$ $(i \leq k)$ and $x_i > 0$ $(k < i \leq n-1)$, and consider

$$\begin{aligned} I_R &= \int_0^1 dx_n f_n(x_1, \ldots, x_n) \\ &= f_k(x_1, \ldots, x_k) \int_0^1 dx_n f_{n-k}(x_{k+1}, \ldots, x_n) \\ &= \left(1 - \sum_{i=k+1}^{n-1} x_i\right) f_{n-1}(x_1, \ldots, x_{n-1}) . \end{aligned} \tag{A19}$$

Using the analog of Eq. (A15) appropriate to the case in which all the x_i are negative, we have also, when $x_i < 0$ $(i \leq k)$ and $x_i > 0$ $(k < i \leq n-1)$,

$$\begin{aligned} I_L &= \int_{-1}^0 dx_n f_n(x_1, \ldots, x_n) \\ &= \int_{-1}^0 dx_n f_{k+1}(x_1, \ldots, x_k, x_n) f_{n-k-1}(x_{k+1}, \ldots, x_{n-1}) \\ &= \left(1 - \sum_{i=1}^{k} |x_i|\right) f_{n-1}(x_1, \ldots, x_{n-1}) . \end{aligned} \tag{A20}$$

The energy-conservation sum rule is

$$\begin{aligned} \int_{-1}^1 dx_n f_n(x_1, \ldots, x_n) &= I_R + I_L \\ &= \left(2 - \sum_{i=1}^{n-1} |x_i|\right) f_{n-1}(x_1, \ldots, x_{n-1}), \end{aligned} \tag{A21}$$

and the longitudinal-momentum sum rule is

$$\begin{aligned} \int_{-1}^1 dx_n \frac{x_n}{|x_n|} f_n(x_1, \ldots, x_n) &= I_R - I_L \\ &= -\left(\sum_{i=1}^{n-1} x_i\right) f_{n-1}(x_1, \ldots, x_{n-1}) . \end{aligned} \tag{A22}$$

---

*Research sponsored by the U. S. Air Force Office of Scientific Research, Office of Aerospace Research, under Contract No. F44620-71-C-0044.

†Alfred P. Sloan Foundation Fellow.

‡Present address: Department of Physics, Columbia University, New York, N. Y. 10027.

[1]See, for example, W. R. Frazer *et al.*, Rev. Mod. Phys. 44, 284 (1972).

[2]A few representative examples are G. Cocconi, Phys. Rev. 111, 1699 (1958); R. Hagedorn, Nucl. Phys. B24, 93 (1970); R. C. Hwa, Phys. Rev. Letters 26, 1143 (1971); M. Jacob and R. Slansky, Phys. Rev. D 5, 1847 (1972).

[3]The "leading-particle" spectrum includes small c.m. momenta so that what we call the leading particle may not actually be leading in all events.

[4]A. Krzywicki and B. Petersson, Phys. Rev. D 6, 924 (1972); B. Petersson, in Proceedings of the Twelfth Rencontre de Moriond (unpublished).

[5]See, for example, Hagedorn, Ref. 2.

[6]This model is a "bootstrap" for particle production once the leading-particle distribution is given. Such a bootstrap perhaps should be called a shoestring.

[7]G. Neuhofer *et al.*, Phys. Letters 37B, 438 (1971); G. Barbiellini *et al.*, *ibid.* 39B, 294 (1972); M. Breidenbach *et al.*, *ibid.* 39B, 654 (1972).

[8]This assumption means that $N_L(\vec{p}, s) \to N_L(x, \vec{p}_\perp)$ as $s \to \infty$. In what follows we assume that the scaling limit of N is obtained by inserting the scaling limit of N_L into Eq. (4). See, however, footnote 14.

[9]Equations (6) are valid if the Lorentz transformation $\Lambda_{p'}$ is a pure boost. If, however, it includes a small rotation (for example, if the longitudinal direction for the fireball decay is defined by the beam direction as seen in the fireball system rather than as seen in the c.m. system), then the function $\vec{k}_\perp(x, y, \vec{p}'_\perp)$ is slightly changed; this change is completely irrelevant when one integrates over transverse momentum.

[10]T. T. Chou and C. N. Yang, Phys. Rev. Letters 25, 1072 (1970); C. E. DeTar, D. Z. Freedman, and G. Veneziano, Phys. Rev. D 4, 906 (1971); E. Predazzi and G. Veneziano, Lett. Nuovo Cimento 2, 749 (1971); L. S. Brown, Phys. Rev. D 5, 748 (1972).

[11]Strictly speaking, Eq. (18) requires the integral to exist in order that $f(0) \neq 0$. This will certainly happen if $g(x)$ is not so singular at $x = 1$ that $\hat{h}(\lambda)$ is not analytic at $\lambda = 0$. This is true in the cases we consider; see, however, footnote 14.

[12]A. H. Mueller, Phys. Rev. D 2, 2963 (1970).

[13]R. C. Brower and John Ellis, Phys. Rev. D 5, 2253 (1972).

[14]There are technical reasons why it is difficult to include diffractive processes within the bootstrap; that is, to allow them to affect $g(x)$. For example, a triple-Pomeranchukon term (with a linear zero and $\alpha_P = 1$) would imply $g(x) \sim [(1-x)\ln^2(1-x)]^{-1}$ as $x \to 1$, which would make the integral in Eq. (18) diverge; hence $f(0)$ would vanish. Also a triple-Regge term consisting of two Pomeranchukons and an f trajectory would contribute nothing to the scaling limit of $g(x)$ for $|x| < 1$, and yet could affect integrals over g, and so affect $f(x)$ through Eq. (11).

[15]M. Le Bellac, Phys. Letters 37B, 413 (1971); John Ellis, J. Finkelstein, and R. D. Peccei, Nuovo Cimento (to be published).

[16]A. Pignotti and P. Ripa, Phys. Rev. Letters 27, 1538 (1971).

[17]H. D. I. Abarbanel, Phys. Rev. D 3, 2227 (1971).

[18]One way to show this is to express this coefficient in terms of integrals over g, by using Eq. (39) for the ratio of B to A, and by recognizing the integral multiplying B as $\hat{f}(1-\alpha_0) = \hat{g}(1-\alpha_0)/[1-\hat{h}(1-\alpha_0)]$.

[19]J. V. Allaby *et al.*, CERN Report No. CERN 70-12, 1970 (unpublished).

[20]L. W. Jones *et al.*, Phys. Rev. Letters 25, 1679 (1970).

[21]For example, H. Bøggild *et al.*, Nucl. Phys. B27, 285 (1971).

PHYSICAL REVIEW D VOLUME 6, NUMBER 9 1 NOVEMBER 1972

Spectral-Function Sum Rules and ω-ϕ Mixing

B. G. Kenny
Research School of Physical Sciences, The Australian National University, Canberra, Australia
(Received 20 April 1972)

In this paper we perform a calculation of the ω-ϕ mixing problem, using the spectral-function sum rules of Weinberg, which is more comprehensive than previous similar calculations. In conjunction with the first sum rule we assume asymptotic nonet symmetry. We use the second sum rule modified by corrections estimated using the Gell-Mann, Oakes, and Renner model of the SU(3)⊗SU(3)-breaking strong interactions. The predictions of the model are in good agreement with experiment where accurate experimental data are available. We indicate how it is possible to reconcile previous competing theories within the more comprehensive framework of our model.

I. INTRODUCTION

Various authors[1] have used the spectral-function sum rules of Weinberg[2] to investigate the problem of ω-ϕ mixing. As data accumulate from electron-positron storage-ring experiments[3] and photoproduction of neutral vector mesons, these theories will be put to a more severe test.

In this paper, we extend the earlier work of Das, Mathur, and Okubo[1] and of Oakes and Sakurai[1] by systematically exploiting the first Weinberg sum rule and the *modified*[4] second Weinberg sum rule. We find that the sum rules alone specify the ω-ϕ mixing angle and, in addition, make several predictions which seem to be in reasonable accord with experiment.

II. FIRST SUM RULE

We take the first sum rule to be of the form

$$\int dm^2[m^{-2}\rho^{(1)}_{\alpha\beta}(m^2) + \rho^{(0)}_{\alpha\beta}(m^2)] = S\delta_{\alpha\beta}$$

$$(\alpha, \beta = 0, \ldots, 8)\,, \quad (1)$$